

# Creep rupture of a phenolic–alumina particulate composite

T. H. SERVICE

*Service Engineering Laboratory, 324 Wells Street, Greenfield, MA 01301, USA*

The creep and creep rupture behaviour of a phenolic–alumina particulate composite was determined in an aqueous environment. Flexural creep tests were carried out in which the loading-point displacement was measured as a function of applied stress and time. The material exhibits power-law creep behaviour in which the steady-state creep rate is a power function of the initial applied elastic stress. The creep exponent was found to be 5.3. The creep rupture behaviour can be explained using a modified Monkman–Grant relationship which provides a failure criterion that is independent of applied stress and stress state.

## 1. Introduction

Polymer composites are common engineered materials that have a wide range of applications. Composites that utilize phenolic resin as a binder are particularly common with applications within the building material industry in plywood and more recently in engineered laminated composite beams. Other widely used applications include those in the friction materials industry as brake pads and liners, the manufacturing industry as material-removing abrasives, and the foundry industry in mouldings as well as numerous uses in the aerospace industry. Phenolic composites are the material of choice in these applications because of their ease of fabrication, high strength to weight ratio and superior behaviour at elevated temperatures.

In many applications, these materials are used as structural load-bearing components and are subjected to various applied stresses and environments. Assuring their long-term reliability and preventing failure requires an understanding of the mechanical behaviour of these materials under the expected operating conditions. It has been known for some time that polymer composites can absorb moisture from the environment which can have a deleterious affect on the mechanical properties [1–3]. More recently, studies have shown how the presence of moisture during the fabrication phase can result in inferior mechanical properties [4, 5]. However, a relative dearth of information exists on the factors which influence the long-term structural reliability of phenolic composites, particularly in aqueous and humid environments. Research on a phenolic–alumina particulate composite [6–8] has shown that when tested in ambient environments, the strength and time-dependent failure behaviour can be explained using linear elastic fracture mechanics theory. However, when tested in an aqueous environment the material exhibits accelerated strength degradation and failure. In these environments a more plausible explanation of this behaviour is a time-dependent creep mechanism.

Therefore, the purpose of this research is to examine the creep and creep rupture behaviour of a phenolic–alumina particulate composite in aqueous environments.

## 2. Experimental procedure

The material examined in this study is a phenolic resin–alumina particulate composite with a microstructure that consists of three basic components: aluminium oxide grit, a phenol–formaldehyde resin binder and porosity. The alumina grit constitutes approximately 50 vol % of the material, the phenolic resin binder constitutes ~ 22 vol % and the remaining 28 vol % is porosity. The bulk density is 21.8 kN m<sup>-3</sup>. The material was fabricated into flexure test specimens with dimensions 150 mm × 25.4 mm × 12.7 mm and were tested in the as-moulded condition.

The creep and creep rupture experiments were carried out in flexure using a fixture that could be varied to obtain three different configurations: three-point flexure, four-point flexure with a loading span of 25.4 mm and four-point flexure with a loading span of 50.8 mm. In all configurations the outer support span was 127 mm. All tests were at a constant load (i.e. bending moment) which was obtained by applying a fixed load to the end of a lever arm which transferred the load to the specimens. The fixture and specimens were submerged in a 23 °C water environment for the duration of the tests.

The time-dependent creep behaviour was obtained by recording the load-point deflection of the bend fixture as a function of time, applied stress and stress state. A linear voltage displacement transducer (LVDT) was attached to the top of the fixture and the displacement of this upper portion was recorded using a strip-chart recorder. Thus, the displacement of the load points was measured relative to the support points. The time to failure of each specimen was also recorded. Tests were carried out at initial elastic stress

ses corresponding to 27.6, 24.1, 20.7, 17.2, 13.8 and 12.4 MPa. Ten specimens were tested at the applied stresses ranging from 27.6 to 17.2 MPa in three-point bending (3-pt) and four-point bending with inner spans of 25.4 and 50.8 mm (referred to hereafter as 4-pt<sub>1</sub> and 4-pt<sub>2</sub>, respectively). In addition, seven and four specimens were tested at applied stresses of 13.8 and 12.4 MPa, respectively in 4-pt<sub>1</sub> bending.

### 3. Results and discussion

#### 3.1. Creep deformation

The results of the load-point deflection tests carried out in 4-pt<sub>1</sub> flexure under stresses ranging from 27.6 to 13.8 MPa are shown in Fig. 1. These results are typical of all of the other tests so only these are shown for clarity. The results show that this material exhibits the typical creep behaviour observed in other materials such as metals and ceramics at elevated temperature. That is, the material shows an initial primary creep region followed by an extended secondary or steady-state creep rate region ending with a short tertiary creep region. Fig. 1 also shows that as the applied stress decreases, the slope of the curve in the steady-state region decreases and the time to failure and deflection at failure increase.

The steady-state creep rate in tension,  $\dot{\epsilon}$ , is typically given as a power function of the applied stress by the Norton relationship [9]:

$$\dot{\epsilon} = \dot{\epsilon}_0 (\sigma_a / \sigma_0)^n = A \sigma_a^n \quad (1)$$

where  $\sigma_a$  is the applied stress,  $\dot{\epsilon}_0$ ,  $\sigma_0$ , and  $A$  are constants and  $n$  is the creep stress exponent. However, creep experiments conducted in flexure have the complication that the specimen is in both tension and compression. Hollenberg [10] first examined the effects of a bending stress state on the creep behaviour of

ceramics. His analysis showed that when the creep behaviour in tension is the same as in compression, the maximum outer fibre strain,  $\epsilon_{\max}$ , is related to the load-point displacement  $y_L$  and the creep parameter  $n$  through the relationship

$$\epsilon_{\max} = \frac{2t(n+1)}{(L-a)[L+a(n+1)]} y_L \quad (2)$$

where  $t$  is the specimen thickness,  $L$  the support span and  $a$  the loading span. Since the strain is a function of the creep exponent  $n$ , this parameter must be determined before the actual creep strain can be calculated.

One way to obtain the creep exponent,  $n$ , from steady-state creep behaviour is to plot the load-point deflection rate,  $\dot{y}_L$ , versus the applied load (or bending moment) on a log-log plot. The result should be a straight line with a slope equal to  $n$ . For the three different test configurations examined in this study there are three parallel linear lines with increasing deflection rates with increasing stressed area, i.e. 4-pt<sub>2</sub> deflects the fastest, 4-pt<sub>1</sub> does not deflect as quickly and the 3-pt deflects the slowest. The slope of each curve was calculated by linear regression and the average of the three was taken to be the creep exponent  $n$  in Equation 1. The results of this analysis give  $n = 5.3$ .

The individual steady-state creep rates for each specimen were then obtained by substituting this value of the creep exponent  $n$  into Equation 2. The average of these creep rates for each test configuration and applied stress is shown in Fig. 2. These results clearly indicate that as the applied stress decreases, the creep rate decreases. More important, the creep rates are independent of bend test geometry in that all of the results fall along a single curve. The excellent agreement between all the different stress states and the linear relationship indicates that this material can be accurately represented by the power law expression given by Equation 1. The slope is taken to be the creep

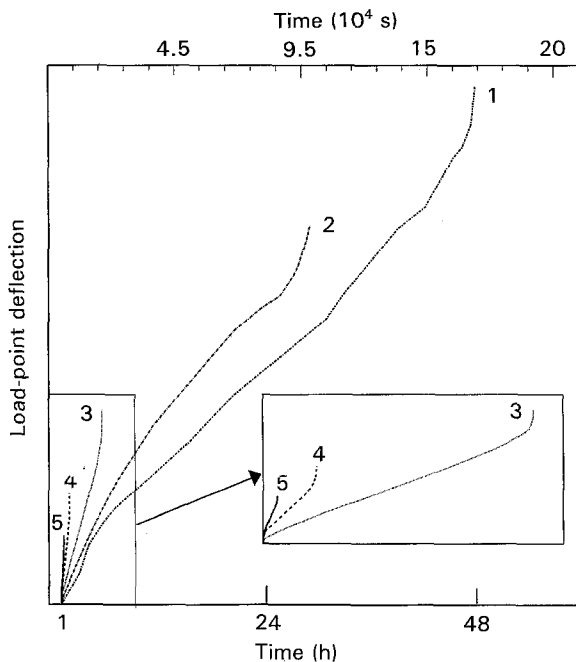


Figure 1 Typical load-point deflection behaviour of a phenolic-alumina particulate composite tested in four-point flexure in an aqueous environment. Applied stress (MPa): (1) 13.8, (2) 17.2, (3) 20.7, (4) 24.1, (5) 27.6.

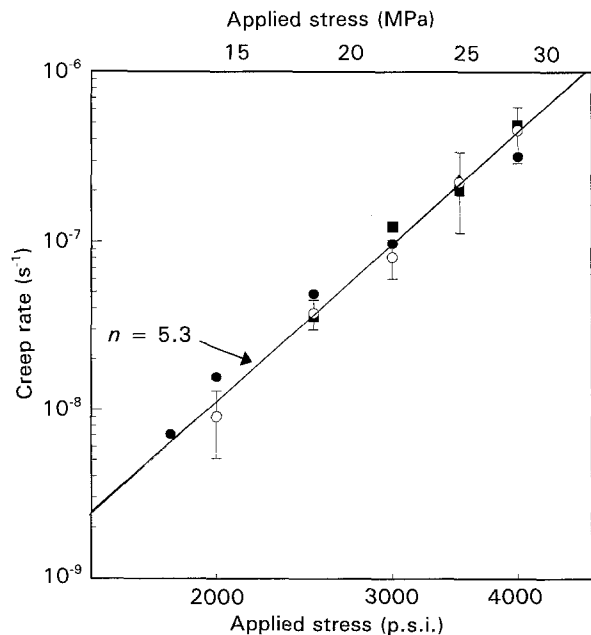


Figure 2 Steady-state creep rate as a function of applied stress: (■) 3-pt, (●) 4-pt<sub>1</sub>, (○) 4-pt<sub>2</sub>.

exponent  $n = 5.3$  as determined earlier and the constant  $A = 1.06 \times 10^{-14}$  is obtained by a least-squares fit to the data with this slope.

In addition to calculating the creep rates, the creep strain at failure was also calculated. As illustrated in Fig. 1, the creep strain at failure increases as the applied stress decreases. These failure strains range from less than 0.25% for specimens tested in 3-pt flexure at 27.6 MPa up to 4% for specimens tested under 4-pt<sub>1</sub> flexure at 12.4 MPa. These relatively small amounts of creep strain at rupture are indicative of the brittle type of failure observed in this material.

Research on fully dense brittle materials such as ceramic composites has shown that the high-temperature creep behaviour can be asymmetrical [11–13]. That is the creep behaviour, and hence the creep parameters, is different in tension and in compression. Typically, these materials exhibit significantly more creep in tension than in compression at the same stress levels. The explanation given for this behaviour is that in tension, creep is controlled by the deformation and cavity formation in secondary phases at grain boundaries, junctions and interfaces; whereas in compression, deformation is mainly in the individual grains where they are in compressive contact. The result of this asymmetric behaviour is that when tested in flexure, the neutral axis no longer remains in the specimen centre line but moves with time off the beam centre. This migration results in time-dependent stress and strain states that are much more complicated and no longer represented by Equation 2. It also means that the creep parameters cannot be readily obtained from flexure experiments but must be determined independently from separate tension and compression tests.

In this material, however, there is considerable porosity and it is likely that the individual grit particles do not directly come into compressive contact with each other. Instead, the grains have the room to move around with relative ease. Therefore, the material may deform as easily in compression as in tension. Based on this observation, all further analyses will be based on symmetrical creep behaviour using Equation 1 to determine the creep strain.

### 3.2. Creep rupture

The creep deformation behaviour illustrated in Figs 1 and 2 shows how the material deforms under stress. However, if these materials are to be used reliably for extended periods of time then it is important to know not only how much the material deforms but if and when the material will fail. It has been suggested that the creep lifetime of many materials can be explained using a Monkman–Grant type of relationship which relates the failure time  $t_f$  to the creep rate  $\dot{\epsilon}$  by [13–19]

$$t_f = C\dot{\epsilon}^{-m} \quad (3)$$

where  $C$  and  $m$  are material and environmental constants. Equation 3 has been shown to be valid for various metals, ceramics and ceramic composites with a single curve being able to describe the behaviour of a

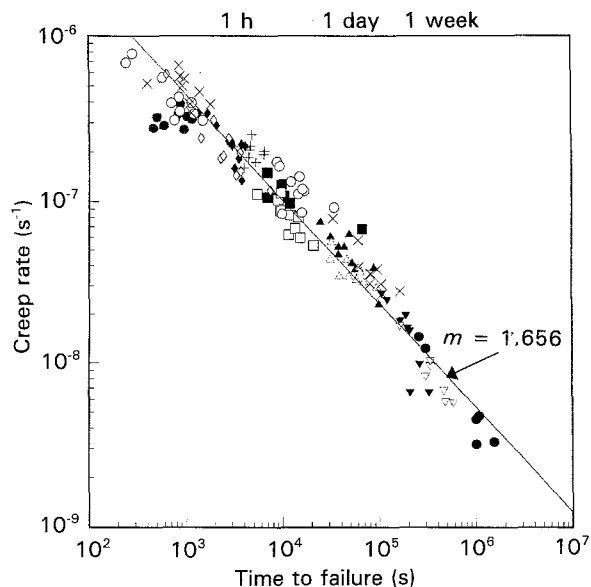


Figure 3 Modified Monkman–Grant Relationship showing steady-state creep rate as a function of time to failure. 3-pt stress (MPa): (×) 17.2, (○) 20.7, (+) 24.1, (x) 27.6. 4-pt<sub>1</sub> stress (MPa): (●) 12.4, (▼) 13.8, (▲) 17.2, (■) 20.7, (◆) 24.1, (⊗) 27.6. 4-pt<sub>2</sub> stress (MPa): (▽) 13.8, (△) 17.2, (□) 20.7, (◇) 24.1, (○) 27.6.

material independent of stress state and temperature. Values for the strain rate exponent  $m$  have been shown to range from 0.77 to 0.93 for metals and between 1.45 and 2.39 for two-phase ceramic composites [18]. An exponent of  $m = 1$  implies a constant strain at failure and assumes that creep in the primary and tertiary stages is negligible, whereas an exponent greater than unity means that the failure strain should increase as the strain rate decreases.

Fig. 3 shows the creep rate as a function of the time to failure for the material examined in this study. In this Monkman–Grant relationship, a regression gives  $m = 1.656$  and  $C = 1.147 \times 10^{-7}$ . This creep exponent greater than unity is consistent with the increased strain at failure at lower strain rates. What is significant about Fig. 3 is that, similar to metals and ceramics, the time to failure is independent of the test geometry and the applied stress. This means that all of the creep rupture data can be explained using this one universal curve, thus providing a criterion for failure.

Two equations can now be used to explain the creep deformation and rupture behaviour of this phenolic–alumina particulate composite in water. Equation 1 describes the creep deformation by relating the creep rate to the applied stress and Equation 3 gives the failure criterion by relating the time to failure to the creep rate. However, a more useful relationship would be one that relates the time to failure to the applied stress. Since the results of this study have shown that the time to failure is independent of the test geometry and stress state and a universal curve gives the failure criteria, Equations 1 and 3 can be combined to give an expression that gives the time to failure as a function of the applied stress:

$$t_f = CA^{-m} \sigma_a^{-mn} \quad (4)$$

Equation 4 shows that if the creep parameters,  $n$  and  $A$ , and the creep rupture parameters,  $C$  and  $m$ , are

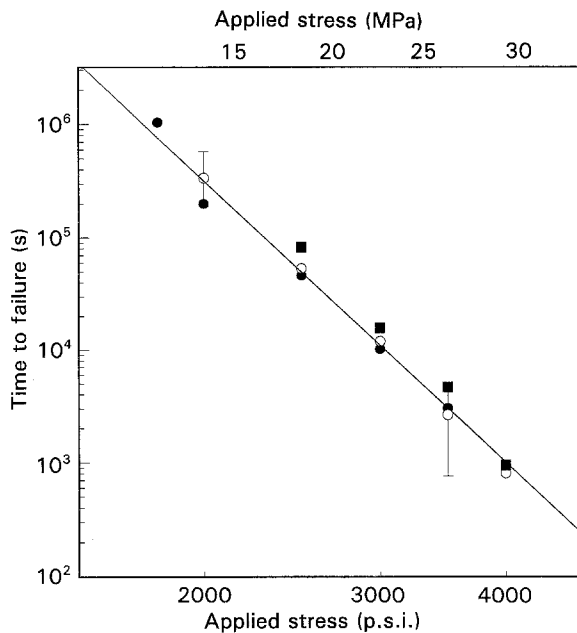


Figure 4 Creep rupture data showing median time to failure as a function of applied stress: (■) 3-pt, (●) 4-pt<sub>1</sub>, (○) 4-pt<sub>2</sub>. The line is a prediction using Equation 4.

known then the time to failure can be predicted. Fig. 4 shows the median times to failure as a function of applied stress for each of the test configurations. Also shown is the predicted curve obtained by substituting for the respective parameters into Equation 4. It should be noted that this curve is not a result of a fit to the data but is predicted from data obtained independently from the creep experiments. Excellent agreement between the data and prediction is evident. While this Monkman–Grant-based relationship does not address the specific mechanism which leads to the delayed failure of this material, it does provide a simple design methodology to make accurate lifetime predictions.

#### 4. Summary

The phenolic–alumina particulate composite material tested in this study exhibits creep behaviour that can be accurately characterized using a power-law relationship between the steady-state creep rate and the

applied stress. Creep rupture lifetimes can be explained using a modified Monkman–Grant relationship which provide a failure criterion independent of applied stress and stress state. A design methodology for predicting creep lifetimes is presented.

#### References

1. L. J. BROUTMAN and R. H. KROCK, in "Modern Composite Materials" (Addison-Wesley, New York, 1967) Ch 2.5.
2. I. K. PARTRIDGE, in "Advanced Composites", edited by I. K. Partridge (Elsevier Applied Science, London, 1989) p. 9.
3. R. DESAI and J. B. WHITESIDE, in ASTM STP 658, edited by J. R. Vinson (American Society for Testing and Materials, Philadelphia, 1978) p. 2.
4. D. S. CHANDRA, R. M. RAO and KISHORE, *J. Mater. Sci.* **10** (1991) 1263.
5. K. JORDON, R. CLINTON and S. JEELANI, *ibid.* **26** (1991) 6016.
6. J. E. RITTER, J. P. FAHEY and T. H. SERVICE, *Trans. ASME, J. Vib. Stress Rel. Design* **108** (1986) 276.
7. J. E. RITTER and T. H. SERVICE, *Mater. Sci. Engng.* **82** (1986) 231.
8. *Idem*, *J. Adv. Ceram. Mater.* **2** (1987) 39.
9. F. H. NORTON, "Creep of Steel at High Temperatures" (McGraw-Hill, New York, 1929) p. 67.
10. G. W. HOLLENBERG, G. R. TERWILLIGER and R. S. GORDON, *J. Amer. Ceram. Soc.* **54** (1971) 196.
11. M. S. SELTZER, *Amer. Ceram. Soc. Bull.* **54** (1977) 418.
12. T. Z. CHUANG, *J. Mater. Sci.* **21** (1986) 165.
13. S. M. WEIDERHORN, D. ELLIS, T. Z. CHUANG and L. CHUCK, *J. Amer. Ceram. Soc.* **71** (1988) 602.
14. R. KOSSOWSKY, D. G. MILLER and E. S. DIAS, *J. Mater. Sci.* **10** (1975) 983.
15. M. K. FERBER, M. G. JENKINS and V. J. TENNERY, *Ceram. Eng. Sci. Proc.* **11** (1990) 1028.
16. S. M. JOHNSON, B. J. DALGLEISH and A. G. EVANS, *J. Amer. Ceram. Soc.* **67** (1984) 759.
17. A. G. ROBERTSON, D. S. WILKINSON and C. H. CACERES, *ibid.* **74** (1991) 915.
18. S. M. WEIDERHORN, B. J. HOCKEY and T. J. CHUANG, in "Toughening Mechanism in Quasi-Brittle Materials", edited by E. P. Shah, (Dordrecht, Boston: Kluwer Academic, Publishers, 1991) p. 555.
19. T. J. CHUANG, D. F. CARROLL and S. M. WEIDERHORN, in "Advances in Fracture Research", Proceedings of 7th International Conference on Fracture, Houston, Texas, March 1989, edited by K. Salama (Pergamon, New York 1989) p. 2965.

Received 2 July 1992  
and accepted 27 April 1993